Substrate Binding and Catalytic Mechanism in Ascorbate Peroxidase: Evidence for Two Ascorbate Binding Sites†

Latesh Lad, Martin Mewies, and Emma Lloyd Raven*

Department of Chemistry, University of Leicester, University Road, Leicester, LE1 7RH, England, U.K.

Received May 20, 2002; Revised Manuscript Received August 27, 2002

ABSTRACT: The catalytic mechanism of recombinant soybean cytosolic ascorbate peroxidase (rsAPX) and a derivative of rsAPX in which a cysteine residue (Cys32) located close to the substrate (L-ascorbic acid) binding site has been modified to preclude binding of ascorbate [Mandelman, D., Jamal, J., and Poulos, T. L. (1998) *Biochemistry 37,* 17610−17617] has been examined using pre-steady-state and steady-state kinetic techniques. Formation ($k_1 = 3.3 \pm 0.1 \times 10^7$ M^{-1} s^{-1}) of Compound I and reduction ($k_2 = 5.2 \pm 0.3 \times 10^6$ M^{-1} s^{-1}) of Compound I by substrate are fast. Wavelength maxima for Compound I of rsAPX (λ_{max} (nm) = 409, 530, 569, 655) are consistent with a porphyrin π-cation radical. Reduction of Compound II by L-ascorbate is rate-limiting: at low substrate concentration (0−500 μM), kinetic traces were monophasic but above ∼500 μM were biphasic. Observed rate constants for the fast phase overlaid with observed rate constants extracted from the (monophasic) dependence observed below 500 μM and showed saturation kinetics; rate constants for the slow phase were linearly dependent on substrate concentration ($k_{3-slow} = 3.1 \pm 0.1 \times 10^3$ M^{-1} s^{-1}). Kinetic transients for reduction of Compound II by L-ascorbic acid for Cys32-modified rsAPX are monophasic at all substrate concentrations, and the second-order rate constant ($k_3 = 0.9 \pm 0.1 \times 10^3$ M^{-1} s^{-1}) is similar to that obtained from the slow phase of Compound II reduction for unmodified rsAPX. Steady-state oxidation of L-ascorbate by rsAPX showed a sigmoidal dependence on substrate concentration and data were satisfactorily rationalized using the Hill equation; oxidation of L-ascorbic acid by Cys32-modified rsAPX showed no evidence of sigmoidal behavior. The data are consistent with the presence of two kinetically competent binding sites for ascorbate in APX.

The ascorbate peroxidase (APX[1]) enzymes are class I (*1*) heme peroxidases which, under physiological conditions, catalyze the H_2O_2-dependent oxidation of ascorbate in plants and algae (*2, 3*). The catalytic mechanism involves formation of an oxidized Compound I intermediate, which is subsequently reduced by substrate in two, sequential single electron-transfer steps, eqs 1−3 (HS = substrate, S• = one-electron oxidized form of substrate):

$$\text{APX} + \text{H}_2\text{O}_2 \xrightarrow{k_1} \text{Compound I} + \text{H}_2\text{O} \quad (1)$$

$$\text{Compound I} + \text{HS} \xrightarrow{k_2} \text{Compound II} + \text{S}^\bullet \quad (2)$$

$$\text{Compound II} + \text{HS} \xrightarrow{k_3} \text{APX} + \text{S}^\bullet + \text{H}_2\text{O} \quad (3)$$

Most APXs are somewhat indiscriminate in their choice of redox partner and are also able to catalyze the oxidation of nonphysiological, aromatic substrates, in some cases at rates comparable to that of ascorbate itself. In this sense, the APX enzymes are similar to the class III, classical peroxidases (*4*) — the most notable member of which is horseradish peroxidase (HRP) — and have provided a useful experimental framework for the examination of the structural determinants of substrate binding specificity in various class I and class III heme peroxidases.

Although crystallographic information is available for the recombinant pea cytosolic APX (rpAPX) enzyme (*5*), there is no structural information on the location of the substrate binding site. The best information available at present comes from two sources. First, NMR-derived distance constraints and molecular modeling work indicated two possible binding sites for ascorbate (*6*): one close to the 6-propionate (γ-meso position) and one close to the δ-meso position of the heme, Figure 1. Second, a series of experiments utilizing a combined mutagenesis/chemical modification approach (*7, 8*) were consistent with an ascorbate binding interaction at the γ-heme edge close to Cys32 and Arg172 (which is close to the γ-meso position implicated by NMR (*6*)). Interestingly, oxidation of classical aromatic substrates, more typical of the class III peroxidase enzymes, were found to be unaffected

† This work was supported by grants from the BBSRC (Special Studentship to LL and Project Grant 91/B11469), the Royal Society (Grants 18851 and 21138), Zeneca, now Syngenta (CASE Award to LL), and the Wellcome Trust (Grant 063688 to E.R.).

* To whom correspondence should be addressed. E-mail: emma.raven@le.ac.uk. Tel: 44 (0)116 252 2099. Fax: 44 (0)116 252 3789.

[1] Abbreviations: APX, ascorbate peroxidase; sAPX, wild-type soybean cytosolic ascorbate peroxidase; rsAPX, recombinant soybean cytosolic ascorbate peroxidase; pAPX, wild-type pea cytosolic ascorbate peroxidase; rpAPX, recombinant wild-type pea cytosolic ascorbate peroxidase; CcP, cytochrome *c* peroxidase; HRP, horseradish peroxidase; sh, shoulder.

10.1021/bi0261591 CCC: $22.00
Published on Web 10/25/2002

FIGURE 1: Structure of rpAPX. The heme, the proximal (His163) and distal histidine (His42) residues, and Cys32 are indicated.

by either removal or modification of Cys32 or removal of Arg172 (*7*, *8*), consistent with the idea that aromatic substrates bind at an alternative location, probably close to the δ-meso position (*6*).

We have initiated a detailed study aimed at dissecting the catalytic mechanism of soybean cytosolic ascorbate peroxidase (sAPX) (*9*−*11*), which has 91% sequence identity with the more well-characterized pea cytosolic enzyme and for which there is currently no mechanistic information. During the course of our analyses, there were two features of the kinetic data that were curious. First, pre-steady-state kinetic transients for reduction of Compound II of rsAPX by ascorbate, eq 3, were observed to be biphasic at high substrate concentrations. Second, steady-state oxidation of ascorbate by rsAPX showed a sigmoidal dependence of rate on substrate concentration and did not conform to normal Michaelis−Menten kinetics. Although this deviation from Michaelis−Menten behavior has been noted previously for this and other APXs (*9*, *10*, *12*), the origin of this behavior is unclear. Since our initial work (*6*) on rpAPX had suggested the possibility of two distinct substrate binding sites, we considered the possibility that this may be responsible for the unusual kinetic behavior. To assess this, we have prepared a derivative of rsAPX in which one of the ascorbate binding sites has been modified (*7*). The data provide the first evidence for the existence of two kinetically competent, ascorbate binding sites in APX.

EXPERIMENTAL PROCEDURES

Guaiacol and 5,5′-dithiobis(2-nitrobenzoic acid) (DTNB) (Sigma Chemical Co.), L-ascorbic acid (Aldrich Chemical Co.) and the chemicals used for buffers (Fisher) were of the highest analytical grade (99+% purity) and used without further purification. Hydrogen peroxide solutions were freshly prepared by dilution of a 30% (v/v) solution (BDH): exact concentrations were determined using the published (*13*) absorption coefficient ($\epsilon_{240} = 39.4\ M^{-1}\ cm^{-1}$).

Recombinant cytosolic soybean APX (rsAPX) was expressed and isolated according to published procedures (*10*). Purified samples of rsAPX showed a single band by SDS−PAGE. Purity was also assessed using the ratio of absorbancies at the Soret and 280 nm peaks: for rsAPX, samples with A_{407}/A_{280} greater than 2.1 were considered pure. Control reactions with recombinant pea cytosolic APX (rpAPX) were also carried out in some cases: rpAPX was purified according to published procedures (*6*) and the purity assessed as above ($A_{403}/A_{280} > 1.9$). Protein concentrations were determined using published absorption coefficients of $\epsilon_{407} = 107\ mM^{-1}\ cm^{-1}$ (*11*) for rsAPX and $\epsilon_{403} = 88\ mM^{-1}\ cm^{-1}$ (*6*) for rpAPX. Specific activities of rsAPX (283 ± 9 units per mg) and rpAPX (256 ± 6 units per mg) were determined according to published procedures (*12*).

Protein modification with Ellman's reagent (5,5′-dithiobis-(2-nitrobenzoic acid)) was according to published procedures (*7*). The integrity of modified samples was confirmed by electrospray mass spectrometry (data not shown). Samples were analyzed using a Micromass Quattro BQ (Tandem Quadrupole) electrospray mass spectrometer. Horse heart myoglobin (Sigma) was used to calibrate the spectrometer in the range 600−1400 *m*/*z*. Protein samples were introduced into the instrument at a flow rate of 5 μL/min. Removal of the trace salt content was achieved using a Centricon-10 concentrator (Amicon) and successive centrifugation and dilution with highly purified water (Elgastat). Samples (∼2 mg/mL, 20 μL) were then diluted 10-fold with a solution of 50:50 (v/v) acetonitrile:water containing 0.1% acetic acid. The electrospray spectrum of rsAPX yielded a mass for the apoenzyme of 28 318.1 ± 0.7 Da, which compares with the theoretical calculated mass of 28 318.62 Da (*6*). The apoenzyme mass of Cys32-modified rsAPX was 28 515.8 ± 0.6 Da: this 197.7 Da increase in mass was consistent with the chemical modification of Cys32 with DTNB (calculated mass increase = 198.17 Da). In control experiments, similar mass increases (a difference of 198.0 Da) were obtained for rpAPX: mass of apo-enzyme = 27 192.8 ± 0.4 Da (calculated mass = 27 192.77 Da); mass of Cys32-modified rpAPX = 27 390.8 ± 0.2 Da.

Transient-state kinetics were performed using a SX.18 MV microvolume stopped-flow spectrophotometer (Applied Photophysics) fitted with a Neslab RTE200 circulating water bath (± 0.1 °C). All experiments were carried out using sodium phosphate buffer, pH 7.0, 5.0 ± 0.1 °C, $\mu = 0.10$ M. For both rsAPX and rpAPX, different batches of enzyme prepared at different times were examined to ensure reproducibility of kinetic transients (also for steady-state kinetics, below). Reported values of k_{obs} are an average of at least three measurements. All kinetic data were analyzed using nonlinear least squares regression analysis on an Archimedes 410−1 microcomputer (Applied Photophysics) using Spectrakinetics software (this uses the Marquardt−Levenberg algorithm). All curve fitting was performed using the Grafit32 software package (Grafit32 version 3.09b, Erithacus Software Ltd.). Pseudo-first-order rate constants for Compound I formation ($k_{1,obs}$) of rsAPX were obtained at 407 nm in single mixing mode by mixing enzyme (0.5 μM) with varying concentrations of H_2O_2. Pseudo-first-order rate constants for Compound I reduction ($k_{2,obs}$) were collected in sequential mixing mode by mixing enzyme (1 μM) with a stoichiometric amount of H_2O_2 (1 μM); after a suitable aging period (∼250 ms), the substrate was then mixed with the solution and reduction monitored at the ferric/Compound II isosbestic point (409 nm for rsAPX and 407 nm for

rpAPX). Pseudo-first-order rate constants for Compound II reduction ($k_{3,obs}$) were measured at the ferric/Compound I isosbestic point (427 nm for rsAPX and 421 nm for rpAPX) according to published procedures (*14*) in single-wavelength mode. In this case, one syringe contained substrate and the other a mixture of enzyme (1 μM) with a stoichiometric amount of H_2O_2 (1 μM) that was allowed to age for two minutes to allow complete conversion to Compound II prior to analysis. To avoid complications from Compound I* formation (*15*), in which protein radical formation has been established in Compound I over longer time scales, an alternative method was used for Compound II reduction (*16*). In this case, 2 μM enzyme was reacted with 2 μM H_2O_2 and 2 μM L-ascorbic acid to obtain authentic Compound II; after a delay of 1 s, the newly formed Compound II was reacted with substrate. Both methods yielded almost identical rate constants (spread of values ± 8%). In control reactions, Compound II reduction was also monitored at the Compound I/II isosbestic (395 nm (rsAPX) or 391 nm (rpAPX)) using both the single mixing and sequential methods (above). Monophasic transient traces were fitted to a single-exponential process, eq 4, to obtain pseudo-first-order rate constants

$$A = Ce^{-k_{obs}t} + b \tag{4}$$

where A is the absorbance change over time, C is a constant related to the initial absorbance, k_{obs} is the observed rate constant, t represents the time in seconds, and b is an offset value to account for a nonzero baseline. Biphasic transients were fitted to a two exponential process, eq 5

$$A = C_1(1 - e^{-k_{obsA}t}) + C_2(1 - e^{-k_{obsB}t}) + b \tag{5}$$

where k_{obsA} and k_{obsB} are the observed rate constants for the fast and slow phases, respectively, C_1 and C_2 are related to the initial absorbance, and b is an offset, again to account for a nonzero baseline. Time-dependent spectra of the various reactions were performed by multiple wavelength stopped-flow spectroscopy using a photodiode array detector and X-SCAN software (Applied Photophysics). Spectral deconvolution was performed by global analysis and numerical integration methods using PROKIN software (Applied Photophysics).

Steady-state measurements (sodium phosphate, pH 7.0, μ = 0.10 M, [enzyme] = 25 nM, 25.0 °C) were carried out according to published protocols (*12*). In brief, in a 1 mL quartz cuvette, varying concentrations of substrate and 25 nM enzyme were preincubated for 3 min in buffer. Reactions were initiated by addition of H_2O_2 (~2.5 μl, ~30 mM) to a final concentration of 0.1 mM: this avoided complications arising from the potential inactivation of rsAPX by preincubation with H_2O_2. In other control experiments (sodium phosphate, pH 7.0, μ = 0.10 M, [enzyme] = 25 nM, 1 mM EDTA), the preincubation step was omitted. Sigmoidal behavior was detected with both methods. Disproportionation of the monodehydroascorbate radical (generated by oxidation of ascorbate) to ascorbate and dehydroascorbate is fast ($k \approx 10^6$ M^{-1} s^{-1} at pH 7.0 (*17*)). The wavelengths and absorption coefficients used for various substrates were as follows: L-ascorbic acid, ϵ_{290} = 2.8 mM^{-1} cm^{-1} (*18*); guaiacol, ϵ_{470} = 22.6 mM^{-1} cm^{-1} (*19*). Data were fitted either to the Michaelis−Menten equation, or to the Hill equation, eq 6

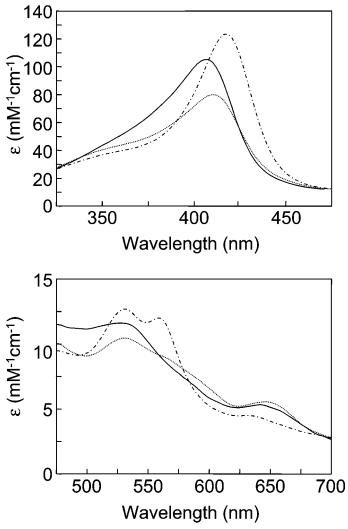

FIGURE 2: Top: UV−visible spectra in the Soret region of ferric rsAPX (solid line) and its oxidized Compound I (dotted line) and Compound II (dashed−dot line) intermediates. Bottom: The corresponding spectra in the visible region.

$$\frac{v}{V_{max}} = \frac{[S]^n}{K^n + [S]^n} \tag{6}$$

where v is the initial rate, n is a qualitative indication of the level of cooperativity, K is the substrate concentration at which the velocity is half-maximal, and V_{max} is the maximum velocity. When $n = 1$, the Hill equation reduces to the more usual Michaelis−Menten equation ($v = V_{max}/(1 + K_M/[S])$).

RESULTS

The spectra of Compounds I and II of rsAPX obtained using photodiode array experiments are presented in Figure 2. Isosbestic points between ferric enzyme and Compound I occur at 427 nm, between Compound I and Compound II at 395 nm, and between ferric and Compound II at 409 nm. The spectrum of Compound I for rsAPX (λ_{max} (nm)/ϵ ($mM^{-1}cm^{-1}$) = 409 (74), 530, 569^{sh}, 655) is similar to those previously published for rpAPX (λ_{max} (nm)/ϵ ($mM^{-1}cm^{-1}$) = 404 (59), 529, 583^{sh}, 650 (*20*)) and pAPX (λ_{max} = 404 nm (*21*)) and provides the first unambiguous evidence for a porphyrin π-cation radical for this intermediate in rsAPX. Wavelength maxima for Compound II (λ_{max} (nm)/ϵ ($mM^{-1}cm^{-1}$) = 417 (119), 529, 560) are essentially identical to that previously reported for rsAPX (λ_{max} (nm) = 418, 527, 561 (*10*)) and for rpAPX (λ_{max} (nm) = 414, 528, 559 (*20*)). Chemical modification of Cys32 of rsAPX resulted in no significant shift in the wavelength maxima for the ferric (λ_{max} (nm) = 407, 516, 636), Compound I (λ_{max} (nm) = 409, 531, 565^{sh}, 656), or Compound II (λ_{max} (nm) = 417, 529, 560) derivatives.

Observed pseudo-first-order rate constants ($k_{1,obs}$) for Compound I formation in rsAPX (data not shown) showed a linear dependence on H_2O_2 concentration. The second-order rate constant, k_1, obtained from the slope of this plot was found to be 3.3 ± 0.1 × 10^7 M^{-1} s^{-1}, which is comparable to that obtained for pAPX (k_1 = 8.0 × 10^7 M^{-1} s^{-1} (*21*)) and rpAPX (k_1 = 6.1 × 10^7 M^{-1} s^{-1} (*20*); k_1 = 8.3 × 10^7 M^{-1} s^{-1} (20 °C) (*7*); k_1 = 9 × 10^7 M^{-1} s^{-1} (*22*)). This rate

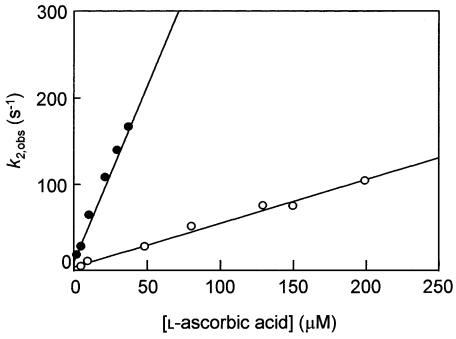

FIGURE 3: Plot of $k_{2,obs}$ vs L-ascorbic acid concentration for the reduction of rsAPX Compound I (●) and Cys32-modified rsAPX (○).

constant for rsAPX was unaffected by chemical modification of Cys32 ($k_1 = 2.8 \pm 0.1 \times 10^7$ M^{-1} s^{-1}).

Reduction of rsAPX Compound I to Compound II was monitored at pH 7.0, the pH optimum for ascorbate activity (*10*). Absorbance−time plots were monophasic in all cases, and a linear dependence of $k_{2,obs}$ on L-ascorbic acid concentration was observed between 0 and 40 μM, Figure 3. The second-order rate constant, k_2, derived from this dependence was $5.2 \pm 0.3 \times 10^6$ M^{-1} s^{-1}, which is slightly lower than the corresponding value obtained for pAPX ($k_2 = 8.2 \times 10^7$ M^{-1} s^{-1} (*21*)) and rpAPX ($k_2 = 2.7 \pm 0.1 \times 10^7$ M^{-1} s^{-1}, this work, data not shown; $k_2 = 3.4 \times 10^7$ M^{-1} s^{-1}, 20 °C (*7*)). For Cys32-modified rsAPX, the corresponding rate constant was $4.4 \pm 0.3 \times 10^5$ M^{-1} s^{-1}: although this value is ~10-fold lower than that for rsAPX itself, it is still too rapid to account for the substantially reduced activity seen in the steady state (vide infra), indicating that the conversion of Compound I to Compound II is not rate-limiting under steady-state conditions.

In contrast to the very rapid reduction of Compound I, reduction of Compound II is relatively slow and is rate-limiting in the mechanism, Figure 4. Between 0 and 500 μM L-ascorbic acid, kinetic traces for rsAPX were satisfactorily fitted to a monophasic profile, Figure 4C, and the dependence of the observed rate constants, $k_{3,obs}$, on substrate concentration showed saturation kinetics, Figure 4A. The total absorbance (amplitude) changes for all monophasic traces (including for rpAPX, vide infra) was between 95% and 98% of the theoretical maximum absorbance change. At L-ascorbic acid concentrations higher than ~500 μM, kinetic traces were biphasic, Figure 4D, and the data were fitted to a two-exponential function, eq 5, which included a fast and slow stage. In control reactions, Compound II reduction was also monitored at the Compound I/II isosbestic using both the single mixing and sequential mixing methods (see Experimental): kinetic transients at both wavelengths using both methods resulted in almost identical kinetic behavior in all cases, eliminating stopped-flow artifacts as a source of the biphasic transients. In further control experiments, the concentration of phosphate (20−500 mM) was found not to affect the kinetic behavior. Observed rate constants for the fast phase ($k_{3,obs-fast}$) of this biphasic process overlaid with observed rate constants, $k_{3,obs}$, extracted from the (monophasic) dependence observed below 500 μM and the entire data set for this stage showed saturation kinetics, Figure 4A. The total change in absorbance (amplitude change) for all biphasic traces (including for rpAPX, vide infra) was between 91% and 97% of the theoretical maximum absorbance change (calculated using the enzyme concentration and the absorption coefficients of the ferric and Compound II spectra). Absorbance changes for the slow stage increased from ~20% to ~30% of the total absorbance change over the concentration range studied. Saturation behavior of this kind is consistent with a mechanism involving preassociation of the substrate (HS) with Compound II, eqs 7 and 8

$$\text{Compound II} + \text{HS} \overset{K_a}{\rightleftharpoons} [\text{Compound II}-\text{HS}] \quad (7)$$

$$[\text{Compound II}-\text{HS}] \xrightarrow{k_{3-fast}} \text{ferric} + \text{S}^{\bullet} \quad (8)$$

and an expression for $k_{3,obs-fast}$ can be derived, eq 9

$$k_{3,obs-fast} = \frac{k_{3-fast}}{1 + K_d/[HS]} \quad (9)$$

where [HS] is the concentration of ascorbate and K_d is the equilibrium dissociation constant for the substrate-bound complex ($K_d = 1/K_a$). A nonlinear fit of the combined data set to eq 9, Figure 4A, yielded values of $k_{3-fast} = 67 \pm 11$ s^{-1} and $K_d = 578 \pm 93$ μM for rsAPX. Observed rate constants for the slow phase, $k_{3,obs-slow}$, were linearly dependent on substrate concentration between 500 and 1000 μM, Figure 4A, and the second-order rate constant, k_{3-slow}, calculated from the slope of the plot was $3.1 \pm 0.1 \times 10^3$ M^{-1} s^{-1}. Similar biphasic kinetic behavior was observed at high substrate concentrations in parallel control experiments on the reduction of Compound II of rpAPX (examined at both 421 and 391 nm using both single- and sequential-mixing methods): in this case, the derived parameters were $k_{3-fast} = 83 \pm 18$ s^{-1}, $K_d = 691 \pm 141$ μM, and $k_{3-slow} = 4.0 \pm 0.1 \times 10^3$ M^{-1} s^{-1}, Figure 4B.

Reduction of Compound II by L-ascorbic acid for Cys32-modified rsAPX is slow and is linearly dependent on substrate concentration without approaching saturation at any accessible substrate concentration, Figure 5. Most important, all kinetic traces are monophasic, even at L-ascorbic acid concentrations greater than 500 μM, Figure 5 (inset). The second-order rate constant, k_3, derived from this linear dependence was $0.9 \pm 0.1 \times 10^3$ M^{-1} s^{-1}. Similar monophasic behavior was observed in control reactions with Cys32-modified rpAPX ($k_3 = 1.4 \pm 0.1 \times 10^3$ M^{-1} s^{-1}). These rate constants are very similar to those obtained from the slow-phase of Compound II reduction for unmodified rsAPX and rpAPX ($3.1 \pm 0.1 \times 10^3$ and $4.0 \pm 0.1 \times 10^3$ M^{-1} s^{-1}, respectively) and are therefore assigned as reporting on the same process.

Steady-state oxidation of ascorbate by rsAPX (sodium phosphate, pH 7.0, $\mu = 0.10$ M, 25.0 °C, [rsAPX] = 25 nM) did not obey Michaelis−Menten kinetics. Plots of initial rate (μM s^{-1}) versus L-ascorbic acid concentration showed a nonhyperbolic (sigmoidal) response, and the data were fitted to eq 6, Figure 6. Values for V_{max}, K, and n derived from these fits were $V_{max} = 6.8 \pm 1.7$ μM s^{-1}, $K = 389 \pm 64$ μM, and $n = 1.5 \pm 0.2$. The pH optimum for steady-state oxidation of ascorbate was at pH ~7 (data not shown). Sigmoidal behavior was also observed in control reactions with rpAPX (data not shown), and the corresponding values derived from a fit of the data for eq 6 were $V_{max} = 6.2 \pm$

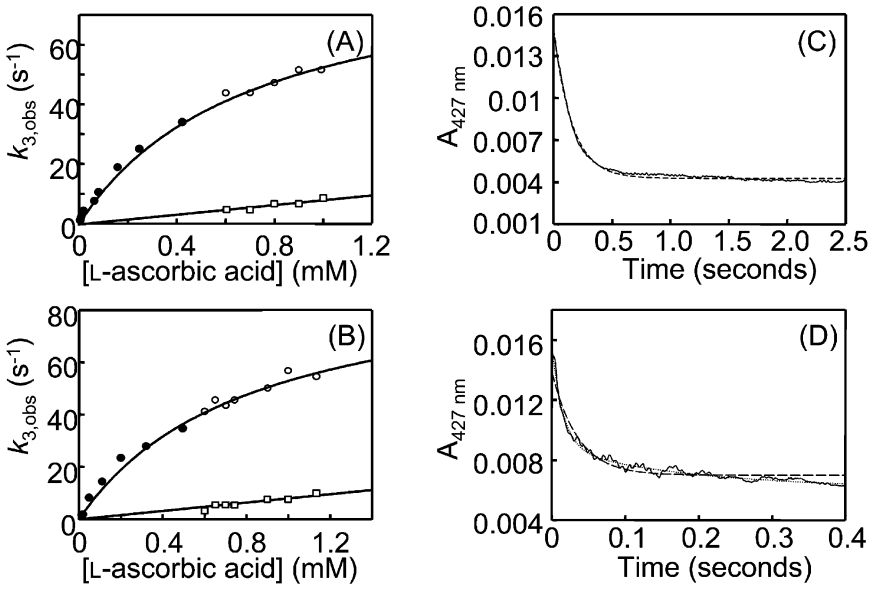

FIGURE 4: (A and B) Plot of observed pseudo-first-order rate constants, $k_{3,obs}$, vs L-ascorbic acid concentration for reduction of (A) rsAPX Compound II and (B) rpAPX Compound II. Rate constants for the fast stage ($k_{3,obs-fast}$) were obtained from monophasic traces at low substrate concentration (●) and from the fast stage of biphasic traces at higher substrate concentration (○); rate constants for the slow stage ($k_{3,obs-slow}$) were obtained from the slow stage of biphasic traces (□). (C) Representative monophasic trace for the reduction of rsAPX Compound II by ascorbic acid (40 μM). The dashed line is a fit of the data to a single-exponential function. (D) Representative biphasic trace for the reduction of rsAPX Compound II by L-ascorbic acid (700 μM). The dotted line is a fit of the data to a two-exponential function, whereas the dashed line is a fit of the data to a single-exponential function.

Table 1: Steady-State Kinetic Parameters and Selectivity Coefficients for the Oxidation of L-Ascorbic Acid and Guaiacol by rsAPX, Cys32-Modified rsAPX, rpAPX and Cys32-Modified rpAPX[a]

		L-ascorbic acid			guaiacol		
enzyme	specific activity (units/mg)	k_{cat} (s^{-1})	K_M (μM)	k_{cat}/K_M[c] ($\mu M^{-1}\ s^{-1}$)	k_{cat} (s^{-1})	K_M (mM)	k_{cat}/K_M[c] ($mM^{-1}\ s^{-1}$)
rsAPX	283 ± 9	272 ± 32[b]	389 ± 64[b]	0.69	68 ± 3	12.9 ± 1.3	5.3
Cys32-rsAPX	11 ± 0.2	–	–	3.5×10^{-3}[d]	59 ± 0.9	16.1 ± 0.4	3.7
rpAPX	256 ± 6	248 ± 28[b]	410 ± 39[b]	0.61	66 ± 3	12.3 ± 0.9	5.4
Cys32-rpAPX	7 ± 0.8	–	–	2.9×10^{-3}[d]	63 ± 2	13.7 ± 1.1	4.6

[a] All data were fitted using the Michaelis−Menten equation, except [b]where data were fitted using the Hill equation. [c] Selectivity coefficients were derived arithmetically from the values for k_{cat} and K_M, except [d]when selectivity coefficients were obtained from a linear fit of the velocity vs substrate concentration profile.

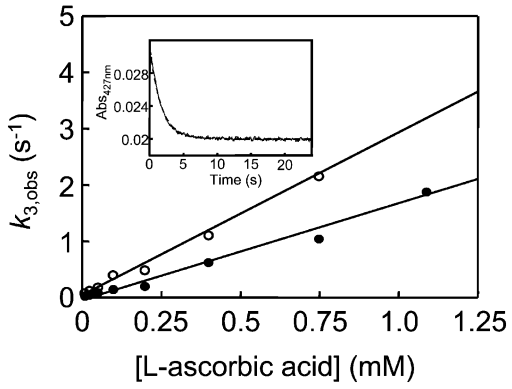

FIGURE 5: Plot of pseudo-first-order rate constants, $k_{3,obs-slow}$, vs L-ascorbic acid concentration for the reduction of the Compound II derivatives of Cys32-modifed rsAPX (●) and Cys32-modified rpAPX (○). Inset: a representative monophasic trace for reduction of Cys32-modified rsAPX ([L-ascorbic acid] = 750 μM]) at 427 nm.

0.7 $\mu M\ s^{-1}$, $K = 410 \pm 39\ \mu M$, and $n = 1.6 \pm 0.7$. At μ = 0.50 M, the same sigmoidal response was observed (data not shown) for both rsAPX and rpAPX, and similar values for V_{max}, K, and n were derived: V_{max}, = 6.1 ± 1.1 $\mu M\ s^{-1}$, $K = 456 \pm 33\ \mu M$, and $n = 1.6 \pm 0.9$ for rsAPX; $V_{max} = 5.8 \pm 0.5\ \mu M\ s^{-1}$, $K = 398 \pm 18\ \mu M$, and $n = 1.6 \pm 0.4$ for rpAPX. In contrast, the oxidation of guaiacol by rsAPX exhibited conventional Michaelis−Menten type kinetics (data not shown). In this case, a fit to the Michaelis−Menten equation yielded values for V_{max} and K_M of 1.71 ± 0.05 $\mu M\ s^{-1}$ and 13 ± 1.3 mM, respectively; the corresponding values for oxidation of guaiacol by rpAPX, which has been previously shown to obey Michaelis kinetics (*7*), were $V_{max} = 1.65 \pm 0.07\ \mu M\ s^{-1}$ and $K_M = 12.3 \pm 0.9$ mM. Values for k_{cat} (derived from V_{max} by dividing the maximum rate of activity ($\mu M\ s^{-1}$) by the enzyme concentration), K_M, and the selectivity coefficient, k_{cat}/K_M, for rsAPX and rpAPX are given in Table 1. Values for k_{cat} for oxidation of ascorbate (25.0 °C) are in reasonable agreement with the limiting rate constants for reduction of Compound II (5.0 °C), with values for k_{cat} ~4-fold higher for both rsAPX and rpAPX. Although other, more complex, kinetic schemes are possible, for example (*23*−*27*), fits of the data obtained in this work to such models did not yield significantly improved fits to the data (not shown).

The steady-state oxidation of L-ascorbic acid by Cys32-modified rsAPX was also examined: rsAPX shows an ~95%

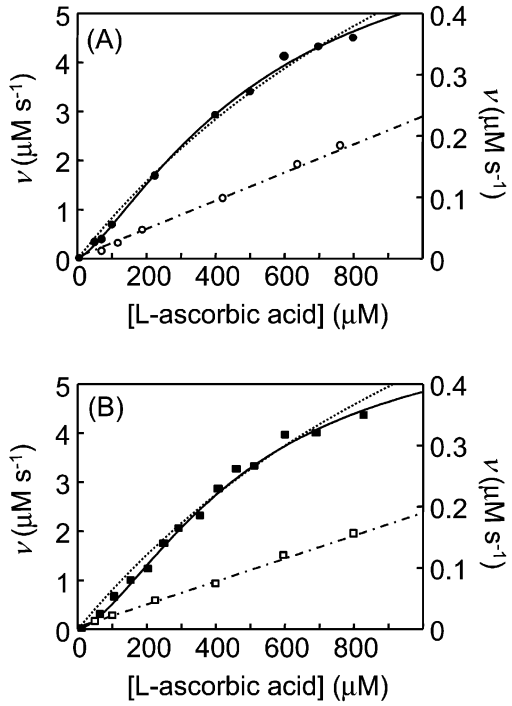

FIGURE 6: Steady-state oxidation of L-ascorbic acid by (A) rsAPX (●, left-hand axis) and Cys32-modified rsAPX (○, right-hand axis) and (B) rpAPX (■, left-hand axis) and Cys32-modified rpAPX (□, right-hand axis). Data were fitted to the Hill equation (solid lines) and to the Michaelis Menten equation (dotted lines). The Cys32-modified rsAPX and rpAPX were fitted to a conventional linear regression (dashed−dot line).

drop in specific activity, Table 1, at 500 μM substrate concentration.[2] The dependence of the initial rate of oxidation (μM s^{-1}) on L-ascorbic acid concentration for Cys32−modified rsAPX is shown in Figure 6. Over the experimentally accessible substrate range (0−800 μM) for this modified protein, a linear profile was observed, with no suggestion of sigmoidal kinetic behavior. As a result of the low activity, a full kinetic profile for Cys32-modified rsAPX could not be generated, and the direct determination of the kinetic parameters (K_M, k_{cat}) was not possible. Instead, selectivity coefficients (k_{cat}/K_M) were obtained directly from the gradient of linear fits to the kinetic profiles, Table 1. The oxidation of guaiacol for Cys32-modified rsAPX was not significantly altered compared to the unmodified enzyme, as has been previously reported for rpAPX (*7*); the derived parameters are shown in Table 1.

DISCUSSION

While mechanistic studies have been a prominent feature of the heme peroxidase literature (reviewed in (*28*−*33*)), our overall understanding of the structural features that define the diverse substrate specificity exhibited by various peroxidases has developed more slowly. The absence of structural information has been at least partly responsible for this: structural information is limited to the complexes formed between cytochrome *c* peroxidase and cytochrome *c* (*34*), between manganese peroxidase and Mn^{2+} (*35*), between horseradish peroxidase and benzhydroxamic acid (*36*) and ferulic acid (including the ternary horseradish peroxidase/cyanide/ferulic acid complex) (*37*), and between myeloperoxidase and its halide (chloride, bromide) substrates (*38*). Although cytochrome *c* peroxidase exhibits rather atypical substrate binding properties—the utilization of a large macromolecular substrate rather than a small organic substrate—the C*c*P enzyme has been the subject of such extensive experimental investigations that it has become the benchmark against which other peroxidase enzymes are often compared. The publication of a crystal structure (*5*) and bacterial expression system (*39*) for another class I peroxidase, ascorbate peroxidase, provided a new opportunity to reassess the properties of C*c*P and to establish in more detail whether it was truly representative of the class I peroxidase subgroup. It later emerged that APX has some rather unexpected features of its own—for example the utilization of a porphyrin-based, not protein-based (as in C*c*P) radical during turnover, a dimeric structure, and unusual steady-state kinetic behavior—that have challenged our existing views of peroxidase structure/function relationships.

In terms of substrate binding, our initial work using NMR-derived distance restraints was consistent with two possible binding locations for ascorbate in rpAPX (*6*): one close to the 6-propionate (γ-meso position) and one close to the δ-meso position of the heme, Figure 1. On the basis of comparisons with other heme peroxidases (e.g., HRP), which use the exposed δ-heme edge for small molecule oxidation (*36*, *37*, *40*−*42*), we initially suggested that the δ-meso site was the more likely location for ascorbate. Subsequently, a series of experiments utilizing a combined mutagenesis/chemical modification approach (*7*, *8*) were used to show that the ascorbate binding interaction was, in fact, at the γ-heme edge in rpAPX, which was close to both Cys32 and Arg172 and to the γ-meso position originally implicated by NMR (*6*). Most notably, oxidation of guaiacol, a classical aromatic substrate, was found to be unaffected by either modification of Cys32 or mutation of Arg172 (*7*, *8*), suggesting that classical aromatic substrates bind at an alternative location, probably close to the δ-meso position identified by NMR and heme modification (*6*). For APX, therefore, the working hypothesis (*6*−*8*) has been as follows. There are two substrate binding locations: the first, close to the γ-heme edge, is utilized by ascorbate; the second, close to the δ-heme position, is utilized by classical aromatic substrates.

During the course of our mechanistic analyses on recombinant soybean cytosolic ascorbate peroxidase, which has 91% sequence identity with the pea enzyme, there were two aspects of the data that were unusual. First, pre-steady-state kinetic transients for reduction of Compound II by ascorbate were biphasic at high substrate concentrations; second, steady-state oxidation of ascorbate by soybean APX showed a sigmoidal dependence of rate on substrate concentration and did not conform to normal Michaelis−Menten kinetics. We considered the possibility that the two substrate binding sites described above were not, in fact, mutually exclusive in APX and might be responsible for the unusual kinetic behavior. As we discuss below, our data suggest that two substrate binding locations are utilized for electron transfer in APX under certain conditions.

[2] For the Cys32-modified enzymes, a linear dependence on substrate concentration was observed and saturation was not detected at any accessible concentration. Hence, specific activities are reported at the same ascorbate concentration which was used to measure the specific activities of (unmodified) rsAPX and rpAPX.

The spectroscopic properties of the Compound I derivative of rsAPX are very similar to those previously observed for rpAPX (*20*) and pAPX (*21*) and provide the first unambiguous evidence for a porphyrin π−cation radical formulation for this intermediate in rsAPX. Although C*c*P is known to form a tryptophan radical at position 191 in its Compound I derivative (*43*−*45*) and although APX contains the corresponding tryptophan residue (Trp179), there is now general agreement from various studies (*15*, *21*, *46*, *47*) that the Compound I species formed immediately after reaction of APX with H_2O_2 contains a porphyrin π-cation radical and not a protein-based radical as observed in C*c*P.

Reduction of Compound II is rate-limiting in the APX mechanism, and our data provide the first unambiguous kinetic evidence for the formation of an enzyme−substrate intermediate prior to electron transfer, followed by rate-limiting reduction of Compound II to ferric at high substrate concentrations, Figure 4. Previous kinetic analyses of Compound II reduction in APX either did not detect limiting kinetics (*21*) or did not fit the (nonlinear) data to any kinetic model (*7*, *8*). While the kinetic transients observed in this work were found to be monophasic at low substrate concentrations, biphasic transients were clearly observed above ~500 μM substrate concentration. Rate constants derived from the fast stage of these biphasic transients overlaid with rate constants derived from monophasic transients at low substrate concentration, clearly indicating that they report on the same process, Figure 4. Most significantly, when rsAPX is modified at the site (close to Cys32) which has been shown (*7*, *8*) to be necessary for ascorbate oxidation, no evidence for biphasic transients is observed and the second order rate constant for Compound II reduction in the modified enzyme is essentially identical to that observed for the slow stage in the unmodified enzyme. These data strongly implicate both high- and low-affinity binding sites for ascorbate, with both sites competent for electron transfer. (The fact that the biphasic dependence is eliminated on modification of the enzyme argues against a mechanism in which two distinct forms of the enzyme—which either interconvert slowly or do not interconvert at all—exist and both react with ascorbate but with different rate constants.) The high-affinity site is close to Cys32 and the γ-heme edge, as implicated previously (*6*−*8*); modification of this site eliminates the high-affinity site and biphasic behavior is not observed. The location of the second, low-affinity site, which is also competent for electron transfer, is less clear but is very likely to be close to the δ-meso position originally implicated by NMR (*6*).

Our results also provide some rationalization for the unusual steady-state behavior exhibited by rsAPX and other APXs. Steady-state analyses have been a fairly prominent feature of the early APX literature (reviewed in ref *2*), and it was noted early on that the oxidation of L-ascorbate by sAPX (*9*), pAPX (*12*), rsAPX (*10*), and rpAPX (*39*, *48*) does not exhibit Michaelis−Menten kinetic behavior, although oxidation of other substrates, for example, guaiacol, does, Table 1. Although there is agreement that sigmoidal behavior is observed when ascorbate is used as substrate, previous kinetic analyses of steady-state data were either not shown (*9*, *10*, *12*, *39*) or, if shown, not fitted to an appropriate model over a suitable concentration range (*7*, *8*, *48*). Our data, Figure 6, show clearly that a Michaelis treatment does not satisfactorily account for the data and show that a fit to the Hill equation is able to satisfactorily account for the data. Although the pea and soybean enzymes are known to exist as homodimers (*5*, *9*), allosteric effects are unlikely to be the source of the sigmoidal kinetics (*48*). In this work, we also observed essentially identical behavior at high ionic strength, also indicating that subunit interactions are unlikely to be responsible for the unusual kinetics. Sigmoidal behavior is also consistent with a mechanism in which binding of substrate at one site induces conformational changes that affect binding of substrate at another: in this case, the observed kinetics will be similar to that observed for an allosteric enzyme (cooperative binding). Our data for both rsAPX and rpAPX are most sensibly rationalized by implicating a model that incorporates cooperative binding involving a second substrate binding site for ascorbate. The positive values ($n = 1.5$ for rsAPX and $n = 1.6$ for rpAPX) for the Hill coefficient derived from this analysis have no physical meaning but do indicate a positive cooperativity in which the affinity of the enzyme for the substrate increases with substrate concentration. Similar analyses have been used to explain the sigmoidal kinetics observed in some cytochrome P450-catalyzed oxidations (*23*, *25*). The 20−30-fold decrease in specific activity, Table 1, for the Cys32-modified derivatives of both rsAPX and rpAPX indicates a dramatically impaired ability to catalyze oxidation of ascorbate in both cases. Most importantly, the Cys32-modifed enzymes show no evidence for a sigmoidal dependence on substrate concentration, providing further support to the hypothesis that the unusual steady-state behavior derives from the existence of more than one substrate binding site for ascorbate.

Taken together, the data presented in this work provide new insight into the substrate binding properties of the APX enzyme. In the wider context of substrate binding and catalysis in other heme peroxidases, it is interesting to note that cytochrome *c* peroxidase (*49*−*56*), manganese peroxidase (*57*), and lignin peroxidase (*58*) have all been shown to have more than one substrate binding site.

ACKNOWLEDGMENT

Mr. John Lamb and Professor Peter Farmer (Centre for Mechanisms of Human Toxicity, Leicester University) are gratefully acknowledged for assistance with mass spectrometric analyses. We thank Mr. Kuldip Singh for technical assistance and Professor Nigel Scrutton and Dr. Jaswir Basran for helpful discussions. Drs. Ian Ashworth and Brian Cox (Syngenta) are gratefully acknowledged for their support of this work.

REFERENCES

1. Welinder, K. G. (1992) *Curr. Opin. Struct. Biol 2*, 388−393.
2. Raven, E. L. (2000) in *Subcellular Biochemistry: Enzyme Catalysed Electron and Radical Transfer* (Holzenberg, A., and Scrutton, N. S., Eds.) pp 318−350.
3. Dalton, D. A. (1991) in *Peroxidases in Chemistry and Biology* (Everse, J., Everse, K. E., and Grisham, M. B., Eds.) pp 139−154, CRC Press, Boca Raton, FL.
4. Heering, H. A., Jansen, M. A. K., Thorneley, R. N. F. and Smulevich, G. (2001) *Biochemistry 40*, 10360−10370.
5. Patterson, W. R. and Poulos, T. L. (1995) *Biochemistry 34*, 4331−4341.

6. Hill, A. P., Modi, S., Sutcliffe, M. J., Turner, D. D., Gilfoyle, D. J., Smith, A. T., Tam, B. M. and Lloyd, E. (1997) *Eur. J. Biochem. 248*, 347−354.
7. Mandelman, D., Jamal, J. and Poulos, T. L. (1998) *Biochemistry 37*, 17610−17617.
8. Bursey, E. H. and Poulos, T. L. (2000) *Biochemistry 39*, 7374−7379.
9. Dalton, D. A., Hanus, F. J., Russell, S. A. and Evans, H. J. (1987) *Plant Physiol. 83*, 789−794.
10. Dalton, D. A., Diaz del Castillo, L., Kahn, M. L., Joyner, S. L. and Chatfield, J. M. (1996) *Arch. Biochem. Biophys. 328*, 1−8.
11. Jones, D. K., Dalton, D. A., Rosell, F. I., and Raven, E. L. (1998) *Arch. Biochem. Biophys. 360*, 173−178.
12. Mittler, R. and Zilinskas, B. A. (1991) *Plant Physiol. 97*, 962−968.
13. Nelson, D. P. and Kiesow, L. A. (1972) *Anal. Biochem. 49*, 474−478.
14. Celik, A., Raven, E. L. and Cullis, P. M. (2000) *Arch. Biochem. Biophys. 373*, 175−181.
15. Hiner, A. N. P., Martínez, J. I., Arnao, M. B., Acosta, M., Turner, D. D., Raven, E. L. and Rodríguez-López, J. N. (2001) *Eur. J. Biochem. 268*, 3091−3098.
16. Kvaratskhelia, M., George, S. J. and Thorneley, R. N. F. (1997) *J. Biol. Chem. 272*, 20998−21001.
17. Kelley, P. M., Jalukar, V. and Njus, D. (1990) *J. Biol. Chem. 265*, 19409−19413.
18. Asada, K. (1984) *Methods Enzymol. 105*, 422−427.
19. Santimone, M. (1975) *Can. J. Biochem. 53*, 649−657.
20. Lad, L., Mewies, M., Basran, J., Scrutton, N. S. and Raven, E. L. (2002) *Eur. J. Biochem. 369*, 3182−3192.
21. Marquez, L. A., Quitoriano, M., Zilinskas, B. A. and Dunford, H. B. (1996) *FEBS Lett. 389*, 153−156.
22. Pappa, H., Patterson, W. R. and Poulos, T. L. (1996) *J. Biol. Inorg. Chem. 1*, 61−66.
23. Miller, G. P. and Guengerich, F. P. (2001) *Biochemistry 40*, 7262−7272.
24. Hosea, N., Miller, G. P. and Guengerich, F. P. (2000) *Biochemistry 39*, 5929−5939.
25. Shou, M., Ettore, M. W., Dai, R., Baille, T. A. and Rushmore, T. H. (1999) *Biochem. J. 340*, 845−853.
26. Ueng, Y.-F., Kuwabara, T., Chun, Y.-J. and Guengerich, F. P. (1997) *Biochemistry 36*, 370−381.
27. Korzekwa, K. R., Krishnamachary, N., Shou, M., Ogai, A., Parise, R. A., Rettie, A. E., Gonzalez, F. J. and Tracy, T. S. (1998) *Biochemistry 37*, 4137−4147.
28. Veitch, N. C. and Smith, A. T. (2001) *Adv. Inorg. Chem. 51*, 107−162.
29. Dunford, H. B. (1999) *Heme Peroxidases*, John Wiley, Chichester, U.K.
30. Dunford, H. B. (1991) in *Peroxidases in Chemistry and Biology* (Everse, J., Everse, K. E., and Grisham, M. B., Eds.) pp 1−24, CRC Press, Boca Raton, FL.
31. Erman, J. E. (1998) *J. Biochem. Mol. Biol. 31*, 307−327.
32. English, A. M. (1994) in *Encyclopedia of Inorganic Chemistry: Iron:haem Proteins, Peroxidases and Catalases* (King, R. B., Ed.) pp 1682−1697, Wiley, Chichester, U.K.
33. Bosshard, H. R., Anni, H. and Yonetani, T. (1991) in *Peroxidases in Chemistry and Biology* (Everse, J., Everse, K. E., and Grisham, M. B., Eds.) pp 51−84, CRC Press, Boca Raton, FL.
34. Pelletier, H. and Kraut, J. (1992) *Science 258*, 1748−1755.
35. Sundaramoorthy, M., Kishi, K., Gold, M. H. and Poulos, T. L. (1994) *J. Biol. Chem. 269*, 32759−32767.
36. Henriksen, A., Schuller, D. J., Meno, K., Welinder, K. G., Smith, A. T. and Gajhede, M. (1998) *Biochemistry 37*, 8054−8060.
37. Henriksen, A., Smith, A. T. and Gajhede, M. (1999) *J. Biol. Chem. 274*, 35005−35011.
38. Fiedle, T. J., Davey, C. A. and Fenna, R. E. (2000) *J. Biol. Chem. 275*, 11964−11971.
39. Patterson, W. R. and Poulos, T. L. (1994) *J. Biol. Chem. 269*, 17020−17024.
40. DePillis, G. D., Sishta, B. P., Mauk, A. G. and Ortiz de Montellano, P. R. (1991) *J. Biol. Chem. 266*, 19334−19341.
41. Miller, V. P., DePillis, G. D., Ferrer, J. C., Mauk, A. G. and Ortiz de Montellano, P. R. (1992) *J. Biol. Chem. 267*, 8936−8942.
42. Wilcox, S. K., Jensen, G. M., Fitzgerald, M. M., McRee, D. E. and Goodin, D. B. (1996) *Biochemistry 35*, 4858−4866.
43. Sivaraja, M., Goodin, D. B., Smith, M. and Hoffman, B. M. (1989) *Science 245*, 738−740.
44. Scholes, C. P., Liu, Y., Fishel, L. A., Farnum, M. F., Mauro, J. M. and Kraut, J. (1989) *Isr. J. Chem. 29*, 85−92.
45. Erman, J. E., Vitello, L. B., Mauro, J. M. and Kraut, J. (1989) *Biochemistry 28*, 7992−7995.
46. Patterson, W. R., Poulos, T. L. and Goodin, D. B. (1995) *Biochemistry 34*, 4342−4345.
47. Kvaratskhelia, M., Winkel, C. and Thorneley, R. N. F. (1997) *Plant Physiol. 114*, 1237−1245.
48. Mandelman, D., Schwarz, F. P., Li, H. and Poulos, T. L. (1998) *Protein Science 7*, 2089−2098.
49. Leesch, V. W., Bujons, J., Mauk, A. G. and Hoffman, B. M. (2000) *Biochemistry 39*, 10132−10139.
50. Mei, H., Wang, K., McKee, S., Wng, X., Waldner, J. L., Pielak, G. J., Durham, B. and Millett, F. (1996) *Biochemistry 35*, 15800−15806.
51. Miller, M. A. (1996) *Biochemistry 35*, 15791−15799.
52. Matthis, A. L., Vitello, L. B. and Erman, J. E. (1995) *Biochemistry 34*, 9991−9999.
53. Zhou, J. S., Tran, S. T., McLendon, G. and Hoffman, B. M. (1997) *J. Am. Chem. Soc. 119*, 269−277.
54. Stemp, E. D. A. and Hoffman, B. M. (1993) *Biochemistry 32*, 10848−10865.
55. Mauk, M. R., Ferrer, J. C. and Mauk, A. G. (1994) *Biochemistry 33*, 12609−12614.
56. Northrup, S. H., Boles, J. O. and Reynolds, J. C. L. (1988) *Science 241*, 67−70.
57. Mauk, M. R., Kishi, K., Gold, M. H. and Mauk, A. G. (1998) *Biochemistry 37*, 6767−6771.
58. Doyle, W. A., Blodig, W., Veitch, N. C., Piontek, K. and Smith, A. T. (1998) *Biochemistry 37*, 15097−15105.

BI0261591